Effect of Mass Transfer on Solid-Catalyzed Reactions: the Dehydrogenation of Cyclohexane to Benzene

L. G. BARNETT, R. E. C. WEAVER, and M. M. GILKESON
Tulane University, New Orleans, Louisiana

The reaction of gaseous components at a solid catalytic surface has long been a subject of prime engineering interest. Generally speaking one expects the reaction velocity constant to follow the Arrhenius exponential temperature dependence. However as the reaction temperature increases, the intrinsic reactivity of the surface will increase and mass transfer begins to limit the rate of the reaction. In the case of a porous solid catalyst, where most of the active surface is on the catalyst pellet interior, the rate-limiting process will frequently be internal diffusion, and in such a case the milder effect that temperature has on the diffusion process is the one observed in the gross kinetics, rather than the exponential Arrhenius dependence.

The study reported here has examined the kinetics of the dehydrogenation of cyclohexane to benzene over a platinum-on-alumina pelleted catalyst. This is a notorious problem system, and in seeking to describe the observed rate data the authors provided a stern test for an analytical model treating the coordinate diffusion and reaction mechanisms. In particular the parameter of particle size was studied over a temperature range of from 640° to 910°F. For these runs reactor pressure was held constant at essentially 200 lb./sq. in. gauge (14.7 atm.), and the feed was maintained at 20 mole % cyclohexane, 80 mole % hydrogen.

BACKGROUND

The catalytic dehydrogenation of cyclohexane to benzene has been studied before, largely because of its relation to petroleum reforming reactions. Weisz and Swegler (*15*) for example considered the kinetics of the production of both benzene and the intermediate cyclohexene over a chromia-alumina catalyst. The present study utilized a platinum-on-alumina catalyst and a range of operating conditions which gave benzene as the only significant reaction product. Only small quantities of the intermediate cyclohexene, with some methylcyclopentane produced by an alternate reaction path, were detected (0.7 mole % maximum).

The analysis used in the present study has been treated previously in the work of Thiele (*12*), Wheeler (*16*, *17*), Wagner (*13*), Zeldowitch (*19*), Weisz (*14*), and Peterson (*8*, *9*). It demonstrates that reacting conditions will exist (notably at higher temperatures and larger catalyst pellet diameters) where there will be a definite bottlenecking effect of the mass transfer rate in the interior of the porous solid on the over-all reaction rate.

Under some of the reaction conditions realized in the present study this phenomenon did occur, and the analytical treatment noted above provided a satisfactory description of the data.

THEORY

The Effect of Intrapellet Mass Transfer on Over-all Kinetics

Wheeler catalogues the relative rates of the diffusion process and the intrinsic chemical processes in terms of an effectiveness factor:

$$E = k_{gx}/k_g \qquad (1)$$

This factor is thus the ratio of actual rate to that which would have been obtained were all of the internal pore walls bathed in the reactant concentration existing at the pore mouths. His analysis draws a straightforward material balance around a differential volume element of a cylindrical pore. Solving the differential equation for isothermal reaction and first-order kinetics, and with boundary conditions precluding an external mass transfer effect, one learns that the effectiveness factor can be expressed in terms of a single dimensionless parameter defined as

$$h = \frac{V_p}{S_x}\sqrt{\frac{k_g}{(1/2)V_g D}} \qquad (2)$$

This definition is a dimensionless modification of the original formulation of Thiele (*12*). Inserting the pellet porosity ($\epsilon = V_g \rho_p$) into the definition and representing the ratio of pellet volume to exterior surface V_p/S_x by $a/6$, one obtains a still more convenient form:

$$h = \frac{V_p}{S_x}\sqrt{\frac{k_g \rho_p}{(1/2)\epsilon D}}$$

$$= \frac{a}{6}\sqrt{\frac{k_g \rho_p}{D_e}} \qquad (2a)$$

Here k_g is the product of the intrinsic surface reactivity and the surface area per gram; it takes the dimensions of volume of space bathed by fluid per unit weight of catalyst per second.

To evaluate h for use in correlation one first computes the diffusivity from molecular properties and appropriate pore radius, temperature, and pressure data. In the present considerations the quantity $[(1/2)\epsilon D]$ appears in this combination throughout the computations and has been replaced with the single symbol D_e. A tortuosity fac-

---

L. G. Barnett is with Humble Oil and Refining Co., Baytown, Texas.

tor has also been incorporated in D_e to account among other things for the fact that the pore path is empirically even more random than the 45° from a beeline predicated by Wheeler. Hoogschagen (*4*) and others have measured tortuosity factors even lower than 0.1 for certain catalyst pellets; a factor of 0.125 has been used in the present study.

Wheeler's solution (*13*) for the effectiveness factor (based on a single pore model) takes the form

$$E = (1/h) \tanh h \qquad (3)$$

Testing the applicability of Equation (3) in the catalytic dehydrogenation system was a prime objective in the present study. Equation (2*a*) allows the computation of the Thiele parameter h once an experimental value of the intrinsic rate constant k_g has been obtained; the latter is obtainable by extrapolation of the Arrhenius plot at lower temperatures where the intrinsic chemical kinetics (which k_g describes), being slow and thus controlling, are represented by the observed rate data. Values of the experimental reactivity k_{gx} at other conditions when compared with the intrinsic constant just discussed result in experimental determinations of the effectiveness factor E [through Equation (1)]. Whether or not the relationship between these experimental measurements of h and E follows the functionality described in Equation (3) constitutes the test for the analytical model.

It is interesting to follow the behavior of the experimental data on a conventional Arrhenius plot of log k_{gx} vs. reciprocal temperature. At the low temperatures, where the intrinsic chemical kinetics control (high values of $1/T$), the expected linear relationship is observed. When the over-all rate becomes subject to the bottlenecking effect of slower internal diffusion rates, for example at high temperatures, the curve bends and approaches unity. In accordance with the model then, effectiveness factor will approach $1/h$; $k_{gx} = E\ k_g$ will thus approach k_g/h. Since h is by definition proportional to $\sqrt{k_g}$

$$k_{gx} \text{ (high temp.) } \sim k_g/h \sim k_g/\sqrt{k_g} \text{ or just } \sqrt{k_g} \qquad (4)$$

Modifications to Account for Poisoning of the Catalyst

Should partial poisoning of the catalyst surface occur, it is possible to modify the form of Equation (3) to take account of this. For a high-activity catalyst surface with which the reaction will take place predominately near the pore mouths the poisoning will take place selectively at these pore mouths. The reactants must subsequently pass through tunnels to reach active surface, and the reaction rate will be limited by the rate of diffusion through these tunnels. The reaction velocity constant will then be a fraction (F_s) of the value which would be observed in the unpoisoned situation. Wheeler (*16*) derives a value for F_s in terms of α, and h_o:

$$F_s = \frac{\tanh[h_o(1-\alpha)]}{\tanh h_o} \cdot \frac{1}{1 + h_o \alpha \tanh[h_o(1-\alpha)]} \qquad (5)$$

Occasion will arise for applying Equation (5) in the present system. As mentioned earlier this process is notorious for its susceptibility to catalyst poisoning. In operation one attempts to suppress the poisoning by conducting the process in a significant hydrogen pressure. While the LeChatelier effect here would tend to repress the main dehydrogenation reaction, the equilibrium is so far to the right that there is no significant effect at low conversions.

APPARATUS AND MATERIALS

The apparatus used for the present study was a continuous benchscale reactor system designed for pressures up to 400 lb./sq. in. gauge and temperatures up to 1,200°F. It consisted of four major sections: hydrogen flow control, oil flow control, reactor complex, and product metering and collection.

Referring to the flow scheme in Figure 1 one may follow the flow of hydrogen feed gas which passed from one of three cylinders through appropriate pressure regulators and flow control and measuring devices to the mixing tee where it met the vaporized oil feed. The cyclohexane, referred to here as "oil," passed through a positive-displacement pump and through control and measuring devices to the vaporizing chamber where it was completely vaporized prior to mixing with the hydrogen feed. The mixture was then fed to the fixed-bed reactor through a preheater. Both the preheater and the reactor were immersed in an isothermal bath which consisted of an electrically-heated fluidized bed.

The reactor itself was a long cylindrical tube, machined from a Type 347 stainless steel billet and fitted with a removable head closure. It was supported at the top by a black iron cover plate which in turn rested on a standard 12-in. pipe. This pipe contained a ceramic cylindrical core wound with 120 ft. of No. 9 gauge Chromel A resistance wire supplying the heat to the fluidized bath within the core. The air for fluidization was supplied through a stainless steel sparger at a superficial velocity of about 0.1 ft./sec. Forty to eighty micron silica particles constituted the fluidized material in the bath.

The product metering and collection system consisted of a vertically mounted, single-pass, water-cooled condenser; a liquid and gas separating space; a graduated liquid collection gauge for batch timing of liquid flow; and a wet test meter. The liquid and gas products were sampled at this point.

Gaseous feed entered the bottom of the reactor billet and passed first through 6 in. of inert packing, where additional preheat was supplied and the velocity profile flattened, and then through layers of catalyst diluted with inerts in progressively decreasing amounts. This aimed at allowing a minimum of temperature drop to give essentially isothermal operation. Longitudinal temperature gradients were measured with a traveling pencil thermocouple mounted inside a steel protection tube.

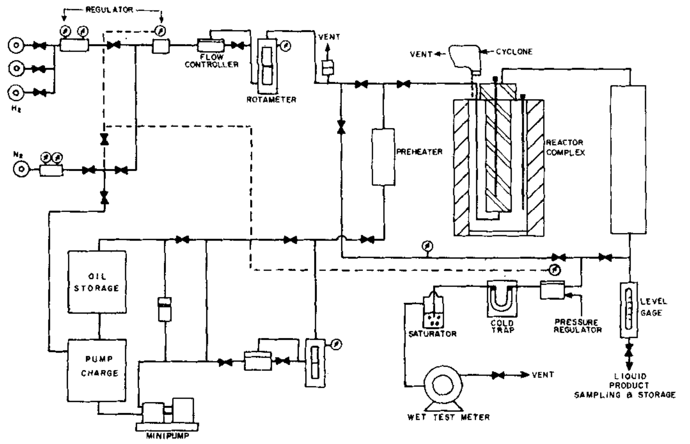

Fig. 1. Diagram of apparatus.

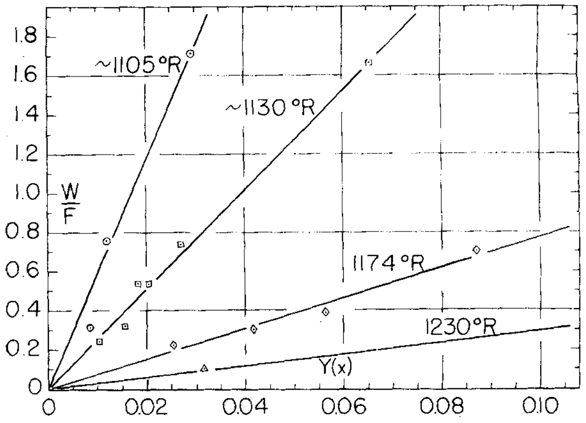

Fig. 2. First-order plot, ⅛-in. pellets.

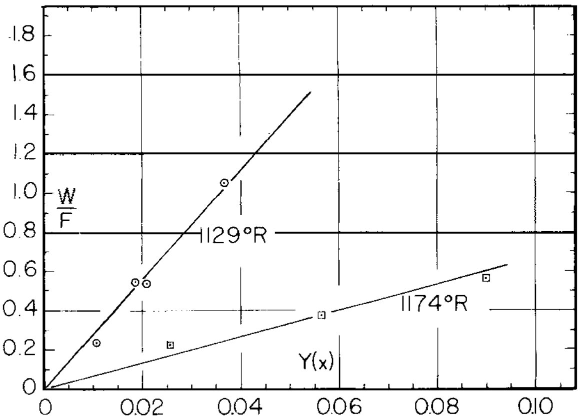

Fig 3. First-order plot, 30- to 40-mesh fines.

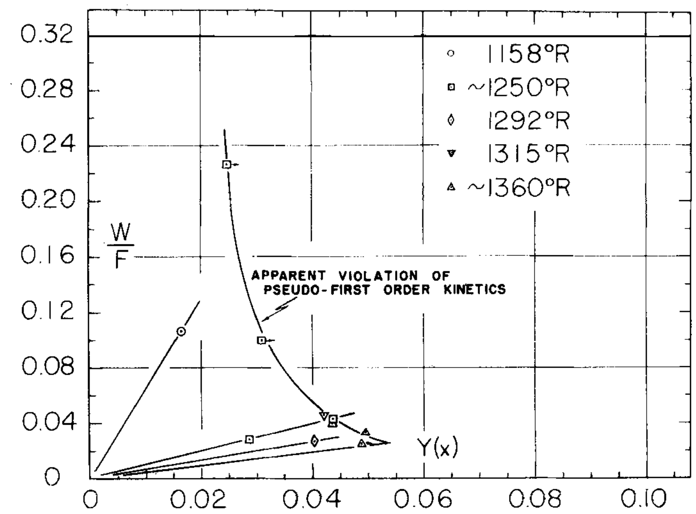

Fig. 4. First-order plot, 40- to 60-mesh fines.

All runs were made in upflow through the bed of pellets or fines; it was not anticipated that this bed would fluidize. As will be pointed out later fluidization or channeling may have occurred in runs with 40-to 60-mesh catalyst fines.

A list of catalyst and feed stock properties is given in Table 4.

PROCEDURE

The reactor was operated on a continuous basis for each of five series of runs. A fresh catalyst charge was used with each series. Runs lasted from 1 to 2 hr., beginning when steady state operation was obtained and ending after sufficient data had been taken.

At the beginning of each series fresh catalyst was charged and leak tests were made. Heat was supplied to the reactor, and a small flow of hydrogen was introduced. To minimize coke formation on the catalyst at elevated temperatures the catalyst was kept in a hydrogen-rich atmosphere. When the desired temperature had been reached (after about 10 hr.), oil flow was introduced and the desired flow conditions were established. Liquid product samples were then taken and immediately analyzed to confirm steady state operation. When all conditions were constant, only two or three consistent analyses were required. Samples were taken every 20 or 30 min. depending on flow rate and were analyzed with a vapor fractometer using a two-meter celite-packed column containing picric acid as the absorbent. Calibrated microdippers were used to inject unknown and standard samples into the helium carrier gas. Gas samples were usually not analyzed since no condensables were obtained in the ice-bathed condensate trap.

To change run conditions flow rates were merely readjusted if the same temperature was to be maintained. To change run temperature oil flow was discontinued, heat input was adjusted, and the temperature was allowed to come to steady state.

EXPERIMENTAL RESULTS

The experimental results are based on detailed data which is presented elsewhere (*1*). Table 1 presents some typical processed data. Material balance information on liquid and gaseous feed and product streams are included to establish the reliability of the flow rate determinations. The results of the first run, Run 10, made with inert packing are presented in Table 1 but do not appear in any of the figures.

These data were then correlated with the conventional flow reactor rate equation into which a first-order expression has been inserted to describe the over-all reaction rate; thus (rate)$\cdot$ $dW = F \cdot dx$. Upon substitution (rate) $= k_{gx} \cdot$ (cyclohexane concentration) and integration conversion x and space velocity W/F are shown to be related as in Equation (6):

$$k_{xg} = \frac{F}{W}[-1.6\ln(1-x) - 0.6x] \qquad (6)$$

The coefficients in the bracketed term apply specifically to a system with feed 0.2 mole fraction cyclohexane. For these experimental conditions then, the equation allows compiling the observed rate data in the form of an over-all reactivity k_{gx}.

The treatment leading to Equation (6) assumes that the reaction proceeds at essentially isothermal conditions. This implies in turn that heat transfer to the catalyst internal surface for the endothermic reaction is a relatively fast process compared with the intrinsic reaction. This situation undoubtedly prevailed at the higher temperatures where the limiting process was internal diffusion. Also in general the experimental work reported here was confined to regimes of low conversion (less than 20%) and should thus conform approximately with the isothermal assumption.

Equation (6) further assumes that the system will display pseudo first-order behavior. Since kinetic expressions in general approach linear behavior at low conversions, it is to be anticipated that the experimental results reported here would conform to this assumption. To test this point specifically, values of W/F were plotted against the term in brackets in Equation (6), referred to as "Y" hereafter. The results are presented in Figures 2 and 3. The linearity of these curves validates the use of the isothermal, pseudo, first-order kinetic model.

The temperature and partial pressure gradients from the bulk gas stream to the pellet interface can be estimated with the *j*-factor correlation (3). Computations for a run made with ⅛-in. pellets at 1,295°R., a case where the external mass transfer effect would be relatively more significant if present, were performed. They show that a cyclohexane pressure gradient of under 1/10 atm. would exist, compared with a bulk gas-phase cyclohexane pressure of 2.9 atm. Also at 1,295°R. the temperature drop from the bulk phase to the catalyst external surface was found to be less than 10°R. For most of the experimental runs reported here this effect would be even less.

If the transfer of heat and mass from bulk fluid to pellet surface in this system had been significant, the effect should have been observable. For in the case of the endothermic dehydrogenation reaction both heat and mass transport to the pellet affect the rate adversely and do not tend to cancel out as in the case of exothermic reactions.

At the low conversions studied here the temperature drop inside the pellet should likewise be small. For the half-dozen runs made at conversions greater than 10% the deviation from Arrhenius' theory is explainable in terms of internal diffusion of the reactant.

The observations on the 40 to 60-mesh fines, presented in Figure 4, show signs of following similar behavior at

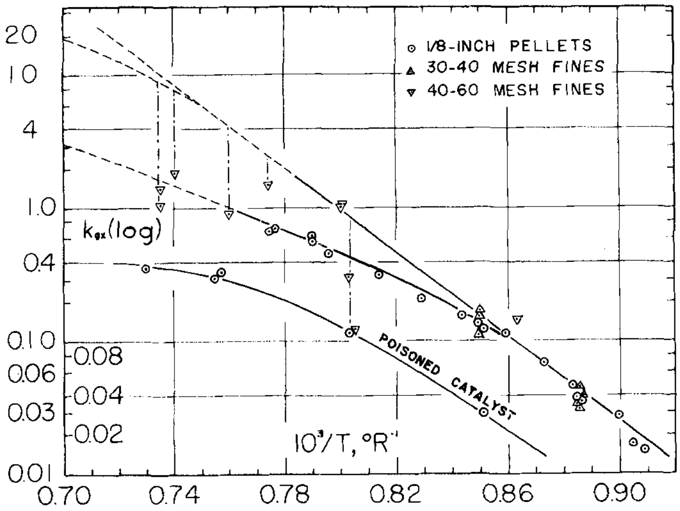

Fig. 5. Arrhenius plot.

lower temperature and/or higher feed rate, but the influence of another parameter is apparent at the higher conversions. This parameter is presumably *an external mass transfer effect*, but as discussed later it could not be handled by the usual *j*-factor correlation.

Values of the logarithm of k_{gx} were plotted against the reciprocal of temperature (in Figure 5) to compare the temperature effect on the reactivity of the system with that predicated by the Arrhenius equation, Equation (7):

$$k_{gx} = A\, e^{-E_0/R_gT} \qquad (7)$$

The low-temperature runs at least would be expected to show this behavior. The activation energy was computed from the slope of the linear portion of the curve at these higher values of reciprocal temperature. It was found to be 41.6 kcal./g. mole.

TEST OF THE EFFECTIVENESS FACTOR MODEL

Equation (2*a*) permits an estimate of the Thiele parameter based on a calculated effective diffusivity and an intrinsic rate constant taken from the experimental data. Further, this constant with the experimentally observed gross rate constant defined in Equation (6) gives the effectiveness factor, Equation (1). This experimental relation between h and E may then be compared with the analytical relationship given by Equation (3).

In calculating the effective diffusivity for travel through a straight pore both bulk diffusivity (for mean free path less than the pore radius) and Knudsen diffusivity (mean free path greater than the pore radius) must be considered coordinately. Wheeler has presented an empirical relation between these two and a net diffusivity. The bulk diffusivities used here were computed from the correlation of Hirschfelder, Bird, and Spotz (*18*). Knudsen diffusivities were computed with a pore volume of 0.48 cc./g. and a surface area of 204 sq. m./g., data which were obtained for the catalyst before and after a run. The mean pore radius was computed to be 43 Å. For a temperature of 1,360°R. D_B was computed to be 0.128 sq. cm./sec. (at 14.7 atm.) and D_K was found to be 0.0134 sq. cm./sec.

Experimental checks of these diffusivities in porous materials however require some consideration of the pore tortuosity. Hoogschagen for example has reported tortuosity factors (χ where $D_e = \chi \epsilon D$) ranging from 0.1 to 0.2. Making use of a degree of freedom in the test of the Wheeler criterion the authors have used the somewhat arbitrary tortuosity factor of 0.125. Based on these considerations then an effective diffusivity of 1×10^{-3} sq.cm./sec. was obtained for cyclohexane diffusing through the 43 Å radius pore at 900°F.

Returning to the test of the model one obtains an estimate of the intrinsic rate constant from the low-temperature linear extrapolation of the Arrhenius plot and this, with the over-all rate constant from the first-order plots, defines *the effectiveness factor*. These values of E and parallel computations of h are tabulated in Table 2 and compared with two models in Figure 6. The upper curve is a plot of Equation (3), $E = h^{-1} \tanh h$; the lower curve is a plot of the equation given below:

$$E = h^{-1}\left[\frac{1}{\tanh 3h} - \frac{1}{3h}\right] \qquad (8)$$

This result derives from Wheeler's rigorous treatment for spherical catalyst granules (*17*).

It will be noted that Figure 6 also presents results from five anomalous runs. Their correlation is discussed next.

Poisoning

The Arrhenius plot for the anomalous series of five runs just mentioned shows a marked decrease in catalyst activity relative to other comparable runs. It was surmised that the catalyst loading in these five runs had been poisoned, probably by a heavy polymer condensed on the catalyst surface at the start of the first run of the series. The early runs in this series were made at the high temperatures, where the reaction would take place predominantly on the pore-mouth surfaces; hence it is likely that whatever poisoning occurred did so selectively at the pore mouths. To test this it is assumed that the fractional activity in the absence of mass transfer (diffusional) effects is measured by the run made at the lowest temperature. Then F_s (the fractional activity) can be computed from the ratio of k_{gx} (poisoned) to k_g (unpoisoned). Thus, based on Run 45, $F_s = (0.032)/(0.15) = 0.22$.

For the limiting case of small values of h_o both homogeneous and selective poisoning correlate simply as

$$F = 1 - \alpha \qquad (9)$$

TABLE 1. SELECTED PROCESSED DATA

Run	Temp., °R.	F^e, cc./sec.	Oil, cc./min. In.	Oil, cc./min. Out	H_2, Std. Mcc./min. In	H_2, Std. Mcc./min. Out	x, C_6H_6	W/F^e, g. sec./cc.	k_{gx}, cc./g. sec.
10[a]	1305	7.07	2.35	2.05	2.05	1.97	0.11	zero	—
11[b]	1267	32.7	12.5	12.65	10.8	10.74	15.5	0.317	0.545
31[c]	1129	32.57	12.55	12.90	10.82	10.25	1.05	0.230	0.046
41[b]	1322	39.0	12.4	12.25	10.80	10.27	1.27	0.039	0.334
45[b]	1175	15.7	5.4	5.0	4.61	4.74	0.31	0.096	0.032
51[d]	1158	14.43	5.4	5.42	5.59	4.89	1.60	0.107	0.152
53[d]	1251	36.0	12.55	12.07	10.60	10.38	4.2	0.043	1.01

Key:

[a] No catalyst used
[b] ⅛-in. catalyst pellets used
[c] 30 to 40-mesh catalyst fines used
[d] 40 to 60-mesh catalyst fines used
[e] The volumetric feed rate has been expressed at 200 lb./sq. in. gauge and reactor temperature.

Table 2. Processed Data for Runs Affected by Internal Diffusion

Run	h	E
11	2.30	0.384
12	3.13	0.266
13	3.12	0.267
14	2.32	0.428
15	2.06	0.41
16	1.50	0.578
17	1.15	0.624
18	0.89	0.83
19	0.64	0.97

Thus α becomes $1 - 0.22 = 0.78$. With this, values of F_s for the four other runs of the series can be computed through Equation (5). The value of k_{gx} for the unpoisoned catalyst can be computed next for each case, since k_{gx} (unpoisoned) is simply k_{gx} (poisoned) divided by F_s. Derived values of h_o, F_s, and the corresponding values of k_{gx} (unpoisoned) are tabulated in Table 3. Values of effectiveness factor are also included here; as corrected for selective pore-mouth poisoning they are shown in Figure 6.

External Mass Transfer

The experimental runs discussed above gave no indication of an effect of external mass transfer. Such was not the case however for the 40 to 60-mesh catalyst fines. Runs made with these under conditions of low mass velocity and/or higher temperature did appear to exhibit such an effect.

Further, the extent of this effect was considerably greater than the usual *j*-factor correlations (*2, 5, 10*) would predict. Kivnick and Hixson (*6*) have reported a similar observation in their study of the reduction of 60- to 200-mesh nickel oxide particles in a fluidized bed. In any event other comparisons of fixed and fluidized bed behavior (*7, 11*) suggest that there may well be a strong effect in the present system attributable to the occurrence of channeling of reactants through the bed, bypassing the catalyst with part of the feed. It was not possible to pursue this point further in the present investigation.

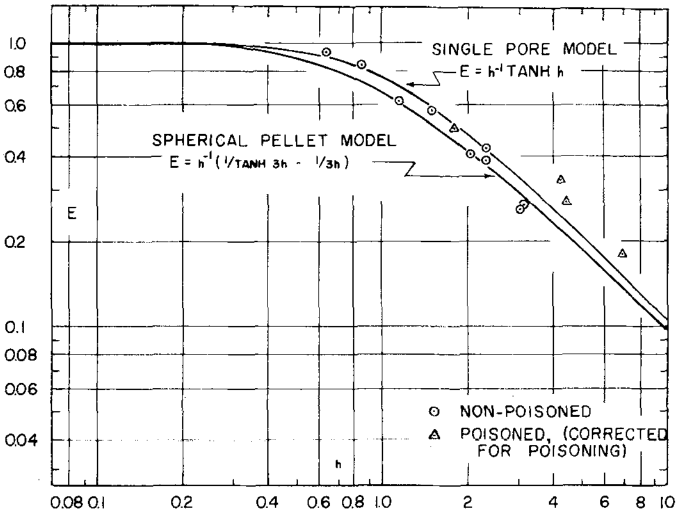

Fig. 6. Catalyst effectiveness.

SUMMARY OF RESULTS

1. In the dehydrogenation of cyclohexane to benzene, at 200 lb./sq. in. gauge pressure and on a platinum-on-alumina catalyst having the properties given in Table 4, the influence of internal diffusion was exhibited by the ⅛-in catalyst pellets above 700°F.

2. The activation energy for the intrinsic catalytic reaction was found to be 41.6 kcal./g. mole. Under internal diffusion control the trend in the data points to an apparent activation energy of half this value.

3. The Wheeler correlation for effectiveness factor as a function of Thiele parameter gave a satisfactory functional model for the system investigated here in which the reaction followed essentially first-order kinetics at low conversions. The best fit to the data resulted when a Knudsen-controlled diffusion coefficient was used with a tortuosity factor of one-eighth to describe the diffusion in the catalyst pores. This value is one-quarter of Wheeler's value which was obtained by assuming that the pores follow a straight-line path making a 45-deg. angle with the external surface of the pellet.

4. The runs on catalyst poisoned inadvertently at the beginning of one series of runs correlated with some measure of success with Wheeler's model for the poisoning of the pore mouths used.

5. The 30- to 40-mesh catalyst fines studied only at the lower temperatures, showed an absence of particle diameter effect. This data supports the postulate that the effectiveness factor for the pelleted catalyst was unity for runs below 700°F.

ACKNOWLEDGMENT

The authors express their appreciation to the American Oil Company and to Ethyl Corporation for fellowship support of this investigation.

NOTATION

A = frequency factor in Arrhenius equation, same dimensions as k_g

Table 3. Processed Data for Runs on Poisoned Catalyst

Run	h_o	F_s	$(k_{gx})_s$*	E_s*
45	0.77	0.22	0.15	1.0
44	1.78	0.26	0.42	0.5
41	4.24	0.214	1.59	0.33
42	4.40	0.210	1.43	0.28
43	6.95	0.153	2.29	0.18

Notes:

* designates that the values have been corrected to unpoisoned equivalents. Subscript *s* designates the use of selective poisoning model.

Table 4. Properties of Materials

Catalyst properties
Pore volume, V_g: 0.48 cc./g.
Surface area, S_g: 240 sq. m./g.
Average pore radius, r: 43 Å.
Pellet density, ρ_p: 1.332 g./cc.
Skeletal density (a measure of the true chemical density where no voids are entrapped and denied access to the exterior): 3.25 g./cc.
Pellet porosity, ϵ: 0.59 cc. voids/cc.

Properties of feed materials
Cyclohexane: Phillips Petroleum Co., commercial pure grade, density (80°F.) = 0.774 impurities consist of 0.7 vol. % other naphthenes, 0.0082 wt. % sulfur.
Hydrogen: Air Reduction Co., electrolytic grade; only impurity is less than 0.1% oxygen.

a = catalyst pellet size (diameter), cm.
D = diffusivity, sq.cm./sec.; D_K = Knudsen diffusion coefficient; D_B = ordinary diffusion coefficient in the bulk gas phase
D_e = effective diffusivity, usually $\chi\epsilon D_B$ or $\chi\epsilon D_K$
E = effectiveness factor
E_o = activation energy in Arrhenius equation
F = flow rate of feed to reactor, cc. at reactor temperature and pressure/sec.
F_s = fractional activity of selectively poisoned catalyst
f = any functional relationship
G = superficial mass velocity, g./sq.cm.sec.
h = Thiele parameter, dimensionless
h_o = Thiele parameter for unpoisoned catalyst; h and h_o can be used interchangeably where poisoning is not a factor
k_g = intrinsic reaction velocity constant, cc. fluid volume/sec./g. of catalyst
k_{gx} = experimentally measured reactivity, same units as k_g
P = pressure
R_g = gas constant, 82.06 cc. atm./g. mole °K.
r = pore radius, usually 2 V_g/S_g, cm.
S_g = specific total catalyst surface area, sq.cm./g.
S_x = external surface area of one catalyst pellet, sq. cm.
T = absolute temperature
V_g = specific internal void (pore) volume, cc./g.
V_p = volume of one catalyst pellet, cc.
W = weight of catalyst in bed, g.
x = moles of cyclohexane converted to benzene per mole of cyclohexane fed
Y = function of x defined by Equation (6), dimensionless

Greek Letters

α = fraction of catalyst surface which is poisoned, dimensionless
ϵ = porosity within a single catalyst pellet, dimensionless
μ = viscosity, g./cm.sec.
ρ = gas density, g./cc.
ρ_p = pellet density of catalyst, g./cc.
χ = tortuosity factor defined above, see D_e

LITERATURE CITED

1. American Documentation Institute, Photoduplication Service, Library of Congress, Washington 25, D. C., document No. 6528, may be obtained for $1.25 for photoprints or for 35-mm. microfilm.
2. Bar-Ilan, Mosche, and William Resnick, *Ind. Eng. Chem.*, 49, 313 (1957).
3. Brown, G. G., *et al.*, "Unit Operations," p. 79, Wiley, New York (1950).
4. Hoogschagen, Jan., *Ind. Eng. Chem.*, 47, 906 (1955).
5. Kettenring, K. N., E. L. Manderfield, and J. M. Smith, *Chem. Eng. Progr.*, 46, 139 (1950).
6. Kivnick, Arnold, and A. N. Hixson, *ibid.*, 48, 394 (1952).
7. Mathis, J. F., and C. C. Watson, *A.I.Ch.E. Journal*, **2**, 518 (1956).
8. Petersen, E. E., *ibid.*, **3**, 443 (1957).
9. *Ibid.*, **4**, 343 (1958).
10. Resnick, William, and R. R. White, *Chem. Eng. Progr.*, **45**, 377 (1949).
11. Shen, C. Y., and H. F. Johnstone, *A.I.Ch.E. Journal*, **3**, 349 (1955).
12. Thiele, E. W., *Ind. Eng. Chem., Analyt. Edit.*, **31**, 916 (1939).
13. Wagner, C. P., *Z. physik. Chem.*, A193, 1 (1943).
14. Weisz, P. B., and C. D. Prator, "Advances in Catalysis,"Vol. 6, pp. 143-196, Academic Press, New York (1954).
15. Weisz, P. B., and E. W. Swegler, *J. Phys. Chem.*, **59**, 823 (1955).
16. Wheeler, Ahlborn, "Advances in Catalysis," Vol. 3, pp. 250-326, Academic press, New York (1950).
17. ———, "Catalysis," Vol. 2, pp. 105-165, Reinhold, New York (1955).
18. Wilke, C. R., and C. Y. Lee, *Ind. Eng. Chem.*, **47**, 1253 (1955).
19. Zeldowitch, J. B., *Acta Phisiochem., USSR*, **10**, 583 (1939).

Manuscript received July 21, 1959; revision received May 6, 1960; paper accepted May 6, 1960. Paper presented at A.I.Ch.E. Kansas City meeting.

Mass Transfer with Liquid Lithium in Circular Conduits

WILLIAM N. GILL, RICHARD P. VANEK, and C. S. GROVE, JR.

Syracuse University, Syracuse, New York

Forced convection mass transfer between circular tubes and liquid lithium was experimentally investigated over a range of Schmidt numbers from 40 to 57 and Reynolds numbers from 5,550 to 22,500. Information concerning the mechanism for mass transfer was obtained by measuring local solution and deposition rates as a function of distance along the tubes. Observed entrance effects for the solution process suggest that it involves the parallel mechanisms of diffusion through a solid film and through occluded liquid in grain boundaries. It is indicated that the relative contributions of these processes changes with increasing temperature.

A j-factor correlation of existing liquid metal mass transfer data for fully developed conditions in circular conduits is presented and indicates that an exponent of 0.112 for N_{Re} best represents the data. This result agrees well with other studies (9).

A number of quantitative studies of mass transfer between turbulent flowing fluids and circular conduits have been made for the purpose of testing and extending the existing theories of mass transfer and also to provide correlations satisfactory for design pur-